12-15-2017

Fluoroethoxy-1,4-diphenethylpiperidine and Piperazine Derivatives: Potent and Selective Inhibitors of [^{3}H]Dopamine Uptake at the Vesicular Monoamine Transporter-2

Emily R. Hankosky
University of Kentucky, erhankosky@gmail.com

Shyam R. Joolakanti
University of Arkansas for Medical Sciences

Justin R. Nickell
University of Kentucky, jnick@uky.edu

Venumadhav Janganati
University of Arkansas for Medical Sciences

See next page for additional authors

Fluoroethoxy-1,4-diphenethylpiperidine and Piperazine Derivatives: Potent and Selective Inhibitors of [^{3}H]Dopamine Uptake at the Vesicular Monoamine Transporter-2

Notes/Citation Information
Published in *Bioorganic & Medicinal Chemistry Letters*, v. 27, issue 24, p. 5467-5472.

Digital Object Identifier (DOI)
https://doi.org/10.1016/j.bmcl.2017.10.039

HHS Public Access

Author manuscript

Bioorg Med Chem Lett. Author manuscript; available in PMC 2018 December 15.

Published in final edited form as:

Bioorg Med Chem Lett. 2017 December 15; 27(24): 5467–5472. doi:10.1016/j.bmcl.2017.10.039.

Fluoroethoxy-1,4-diphenethylpiperidine and piperazine derivatives: Potent and selective inhibitors of [^{3}H]dopamine uptake at the vesicular monoamine transporter-2

Emily R. Hankosky[a], **Shyam R. Joolakanti**[b], **Justin R. Nickell**[a], **Venumadhav Janganati**[b], **Linda P. Dwoskin**[a], and **Peter A. Crooks**[b]

[a]Department of Pharmaceutical Sciences, College of Pharmacy, University of Kentucky, Lexington, KY 40536, USA

[b]Department of Pharmaceutical Sciences, College of Pharmacy, University of Arkansas for Medical Sciences, Little Rock, AR 72205, USA

Abstract

A small library of fluoroethoxy-1,4-diphenethyl piperidine and fluoroethoxy-1,4-diphenethyl piperazine derivatives were designed, synthesized and evaluated for their ability to inhibit [^{3}H]dopamine (DA) uptake at the vesicular monoamine transporter-2 (VMAT2) and dopamine transporter (DAT), [^{3}H]serotonin (5-HT) uptake at the serotonin transporter (SERT), and [^{3}H]dofetilide binding at the human-ether-a-go-go-related gene (hERG) channel. The majority of the compounds exhibited potent inhibition of [^{3}H]DA uptake at VMAT2, with Ki values in the nanomolar range (K_i = 0.014–0.073 μM). Compound **15d** exhibited the highest affinity (K_i = 0.014 μM) at VMAT2, and had 160-, 5-, and 60-fold greater selectivity for VMAT2 vs. DAT, SERT and hERG, respectively. Compound **15b** exhibited the greatest selectivity (>60-fold) for VMAT2 relative to all the other targets evaluated, and **15b** had high affinity for VMAT2 (K_i = 0.073 μM). Compound **15b** was considered the lead compound from this analog series due to its high affinity and selectivity for VMAT2.

Graphical Abstract

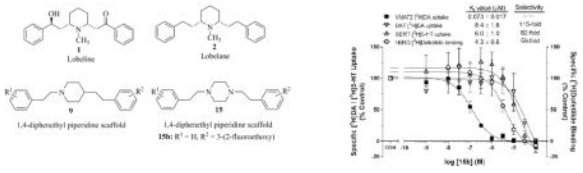

Keywords

Lobelane; Fluoroethoxy piperidine and piperazine analogs; VMAT2; Dopamine uptake; hERG

Psychostimulant use disorders are serious and escalating problems globally, and methamphetamine (METH) is one of the most addictive psychostimulant drugs of abuse[1], causing dopaminergic neuronal damage in humans following long-term METH use.[2] METH use disorders result in severe health consequences, including mood disturbances, infectious diseases (e.g., HIV and hepatitis C), cardiovascular complications, oral disease, and death.[3–7] Currently, there are no FDA-approved drugs for the treatment of METH use disorder.

The vesicular monoamine transporter-2 (VMAT2) plays a major role in mediating the neurochemical and behavioral effects of psychostimulants.[8] VMAT2 is recognized as an important target for the discovery of therapeutics for METH use disorder.[9] Small molecules that modulate VMAT2 function and inhibit the pharmacological effects of METH may prove to be efficacious pharmacotherapies for METH use disorder. In this respect, lobeline (**1**, Fig. 1), the major alkaloid of *Lobelia inflata*, has been shown to inhibit dopamine (DA) uptake into synaptic vesicles via an interaction with VMAT2.[10,11] Evaluation of lobeline's effects in clinical trials revealed some minor side-effects, including bitter taste and nausea, likely the result of an action as an antagonist at nicotinic acetylcholine receptors (nAChRs).[12,13] Another limitation was the short plasma half-life of lobeline (~50 min in rodents),[14] which would require the administration of multiple doses per day to maintain efficacy, and multiple dosing would likely result in diminished compliance.

Our research program set out to identify analogs with enhanced affinity and selectivity for VMAT2. The structure of lobeline was modified to remove the oxygen functionalities, resulting in the symmetrical molecule, lobelane (**2**, Fig. 1). Lobelane exhibited high affinity (K_i = 0.045 μM) for inhibition of [^{3}H]DA uptake at VMAT2 with 43-, 35-, and 2.5-fold greater selectivity for VMAT2 relative to DAT, SERT, and hERG respectively.[11,15,16,21] Moreover, lobelane dose-dependently decreased METH self-administration in rats, without decreasing sucrose-maintained responding, revealing behavioral specificity and affording enhanced potential as a novel treatment for METH use disorder.[17]

Lobelane was modified further to provide two families of analogs, one based on a 2,6-disubstituted piperidine scaffold and another incorporating a 1,4-disubstituted piperidine scaffold, both of which afforded potent inhibitors of DA uptake at VMAT2.[18,19] To further evaluate structure activity relationships around these scaffolds, 1,4-diphenethylpiperidine and 1,4-diphenethylpiperazine analogs have been modified to incorporate aromatic fluoroethoxy moieties. Incorporation of fluorine atoms into strategic positions in a drug molecule can improve electronic and metabolic properties. In addition, fluorinated analogs incorporating an ^{18}F positron-emitting isotope have additional value as potential ligands for positron emission tomography (PET) studies. Also, the substitution of the piperidine moiety with a piperazine moiety in these molecules also may afford improved drug-likeness properties.

Fluoroethoxy-containing 1,4-diphenethylpiperidine derivatives were synthesized starting with benzaldehyde. As illustrated in Scheme 1, a variety of variously substituted benzaldehydes (**3**) were reacted with 4-picoline (**4**) via Aldol condensation in acetic anhydride at reflux temperature to afford the corresponding (*E*)-4-styrylpyridine (**5**). Compound **5** then was hydrogenated with Adams catalyst (PtO_2) in acetic acid under

hydrogen gas (50 psi) at room temperature to afford the corresponding 4-phenethylpiperidino intermediate (**6**). Intermediate **6** was alkylated with various substituted phenethyl bromides (**7**) in the presence of K_2CO_3 in acetonitrile at reflux temperature to yield the corresponding 1,4-diphenethylpiperidine analogs **8a–8k**; these compounds were further *O*-alkylated utilizing ethylfluorotosylate and Cs_2CO_3 in DMF at reflux temperature to yield the corresponding fluoroethoxy-substituted 1,4-diphenethyl-piperidine derivatives **9a–9k** (Scheme-1).

As illustrated in Scheme 2, the fluoroethoxy-substituted 1,4-diphenethylpiperazine derivatives were synthesized starting from 1,4-piperazine. 1,4-Piperazine (**10**) was reacted with a variety of substituted phenethylbromides (**11**) in toluene at reflux temperature to afford 1-phenethylpiperazine (**12**), which was alkylated with various hydroxyphenethylbromides using K_2CO_3 in acetonitrile at reflux temperature, to yield the corresponding 1,4-diphenethylpiperazine analogs **14a–14f**. These compounds were *O*-alkylated utilizing ethylfluorotosylate and Cs_2CO_3 in DMF at reflux temperature to yield the corresponding fluoroethoxy-substituted 1,4-diphenethylpiperazine derivatives **15a–15f** (Scheme 2).

All synthesized compounds were fully characterized by ^{1}H NMR, ^{13}C NMR and high resolution mass spectral analysis.

Compounds **9a–9k** and **15a–15f** were evaluated for inhibition of [^{3}H]DA uptake at VMAT2 and DAT, [^{3}H]5-HT uptake at the serotonin transporter (SERT), and affinity for the human ether-ago-go related gene (hERG) channel to determine cardiotoxicity. The results are provided in Table 1.

For inhibition of VMAT2 function, the [^{3}H]DA uptake assay was conducted using preparations of isolated synaptic vesicles from rat brain.[8,20] The majority of the analogs exhibited K_i values in the nanomolar range (K_i = 0.014–0.073 μM) for inhibition of VMAT2 function. Compound **15d**, 1-(2-chlorophenethyl)-4-(2-fluoroethoxyphenethyl)piperazine, was the most potent inhibitor of [^{3}H]DA uptake at VMAT2, exhibiting a K_i value of 0.014 μM and exhibiting 3-fold greater affinity for VMAT2 compared to lobelane (K_i = 0.045 μM). Compound **15d** exhibited 160-, 5-, and 60-fold greater selectivity for VMAT2 versus DAT, SERT, and hERG, respectively.

Other notably potent compounds in this series were 1-(2-fluoroethoxy)phenethyl)-4-(4-fluorophenethyl)piperazine (**15e**), 4-(2-fluoroethoxy)phenethyl)-1-(2-ethoxyphenethyl)piperidine (**9e**), 4-(2-fluoroethoxy)phenethyl)-1-(4-fluorophenethyl)piperidine (**9h**) and 1-(3-fluoroethoxy)phenethyl)-4-phenethyl piperidine (**9k**), which exhibited inhibition of [^{3}H]DA uptake at VMAT2 with K_i values ranging from 0.024–0.027 μM. Two other compounds, 4-(2-fluoroethoxy)phenethyl-1-phenethylpiperidine (**9d**) and 1-(2-fluoroethoxy)phenethyl-4-phenethylpiperazine (**15a**), also exhibited high affinities for VMAT2 (K_i's = 0.035 μM), which were similar to that for lobelane.

In the 1,4-substituted piperidine series, compounds **9j** and **9k** are positional isomers. Compound **9k**, a 1-(3-fluoroethoxyphenethyl) analog, exhibited 6-fold higher affinity (K_i =

0.024 μM) when compared to **9j**, the 1-(4-fluoroethoxyphenethyl) analog, in the VMAT2 assay. *Ortho*- and *meta*-fluoroethoxylphenyl analogs exhibited generally exhibited greater potency compared to *para*-fluoroethoxyphenyl analogs. Similarly, in the 1,4-piperazine series, compounds **15a**, **15b**, and **15c** are all positional isomers involving the fluoroethoxyphenyl group. Compound **15a**, a 2-fluoroethoxyphenethyl-containing analog, and compound **15b**, a 3-fluoroethoxyphenethyl-containing analog, exhibited high affinity for VMAT2 (K_i = 0.035 and 0.073 μM, respectively), whereas compound **15c**, a 4-fluoroethoxyphenethyl-containing analog, was 8- to 17-fold less potent than its positional isomeric analogs, **15a** and **15b**. Compound **15d**, containing a 2-fluoroethoxyphenethyl moiety, had the highest affinity (K_i = 0.014 μM) for VMAT2 in this series of analogs.

Interestingly, **15f**, which contains a 4-fluoroethoxyphenethyl moiety, was 32-fold less potent than **15d**. Thus, regiospecificity of the aromatic fluoroethoxy substituent plays an important role in influencing the affinity of these inhibitors for VMAT2.

Evaluation of **9a–9k** and **15a–15f** as inhibitors of [^{3}H]DA uptake at DAT afforded K_i values in the range of 1.06–8.38 μM (Table 1), indicating that these compounds have good selectivity for VMAT2 over DAT. In the SERT assay,[20] K_i values were in the range of 0.070 μM to 6 μM (Table 1). Thus, for the majority of the compounds in this series, good selectivity for VMAT2 over SERT also was found. While **15d** was the most potent (K_i = 0.014 μM) compound in the series as an inhibitor of VMAT2, **15d** exhibited 160-fold and 5-fold selectivity for VMAT2 over DAT and SERT, respectively. Thus, **15d** was one of the least selective compounds in the series.

Compounds **9a–9k** and **15a–15f** were evaluated also for affinity at the hERG channel to determine potential cardiotoxicity.[21] Although the majority of the analogs exhibited moderate affinity for hERG (K_i = 0.28–0.85 μM), most had at least 10-fold greater selectivity for VMAT2 relative to hERG. However, inclusion of a piperazine ring, rather than a piperidine ring in the scaffold, while having minimal impact on affinity for VMAT2 and DAT (as evidenced in comparing **9j** with **15c**, and **9k** with **15b)**, resulted in markedly greater selectivity for VMAT2 over SERT and hERG. These findings suggest that the piperazine-containing scaffold has important advantages with respect to off-target activity (e.g., cardiotoxicity) relative to the piperidine-containing scaffold in the pursuit of potent and selective VMAT2 inhibitors as therapeutics for METH use disorder.

We carried out *in silico* evaluation of several drug-like and physicochemical properties of the above fluoroethoxy analogs and compared them to those of their parent compounds (i.e. molecules in which the fluoroethoxy moiety has been replaced with a methoxy group) utilizing appropriate predictive algorithms (ACD Profiler Suite); these properties included LogP, water-solubility, pKa, Lipinski compliance, drug-likeness, and ADME profiling (Caco-2, CNS penetration, and human intestinal absorption). The fluoroethoxy-1,4-diphenethylpiperidine and piperazine analogs generally exhibited good lipophilicity with logP values in the range of 5.21–5.80 and 3.91–4.56, respectively, and had moderate to good water-solubility (0.41–6.14 and 0.37–3.70 mg/mL, respectively). The piperidine analogs exhibited pKa values in the range 9.1–9.3, whereas the piperazine analogs had pKa values in the range 7.4–7.8. Lipinski compliance and drug-likeness were moderate (1 violation) for

the piperidine analogs and moderate to good (0–1 violations) for the piperazine analogs. The ADME profiling data indicated that both the piperidine and the piperazine analogs were predicted to be highly absorbed (100%) from the human intestine, to be highly permeable in the Caco-2 cell assay, and were classified as CNS penetrants. These data are provided in Tables S1 and S2 in the Supporting Information. Comparison of the above properties of the fluoroethoxy-1,4-diphenethyl piperidine and piperazine analogs with those of their corresponding parent methoxy analogs indicated that replacing the aromatic methoxy substituent with an aromatic fluoroethoxy substituent had little overall effect on these properties.

Compound **15b** was considered the lead compound based on its high affinity for VMAT2 and due to it having the greatest selectivity for VMAT2 in the compound series (Fig. 2, Table 1). Compound **15b** had a K_i value of 0.073 μM for VMAT2 and exhibited 115-, 82-, and 59-fold greater selectivity for VMAT2 compared to DAT, SERT and hERG, respectively. Based on these characteristics, **15b** selectively interacts with VMAT2 and is predicted to have low abuse liability and cardiotoxicity.

In Summary, a small library of fluoroethoxy-containing analogs of 1,4-diphenethylpiperidine and 1,4-diphenethylpiperazine were synthesized and evaluated for inhibition of VMAT2 function, as well as for inhibition of DAT and SERT function and interaction with the hERG channel. The parent compound, lobelane, has a high affinity (K_i = 0.045 μM) for VMAT2 with 43-, 35-, and 2.5- fold greater selectivity relative to DAT, SERT, and hERG respectively. Most of the compounds tested in this study exhibited affinity for VMAT2 (K_i <0.075 μM), similar to lobelane.

Most of the compounds tested in this study exhibited affinity for VMAT2 (K_i <0.075 μM), similar to lobelane. However, many of the compounds exhibited improved selectivity for VMAT2 relative to DAT (45- to 160-fold), SERT (46- to 161-fold), and hERG (11- to 156-fold). Generally, the piperazine and piperidine scaffolds confer affinity at VMAT2 similar to lobelane, while improving selectivity over off target proteins. Notably, the piperazine scaffold may be beneficial for reducing cardiotoxicity.

Compound, **15d** exhibited the highest affinity (K_i = 0.014 μM) at VMAT2 relative to the other compounds in the series; however, **15d** was not selective for VMAT2, exhibiting only 5-fold greater selectivity for VMAT2 versus SERT. Among the compounds in this series, **15b** was the most selective compound for VMAT2, with good affinity (K_i = 0.073 μM) at VMAT2 and 115-, 82-, and 59-fold greater selectivity for VMAT2 relative to DAT, SERT, and hERG, respectively. In particular, it was observed that the piperazino analogs generally exhibited lower affinity for the hERG channel when compared to their piperidino counterparts.

Compound **15b** is considered the lead compound from this series of analogs due to its nanomolar affinity at VMAT2, as well as its >60-fold selectivity for VMAT2 over other the off target proteins. Currently, **15b** is being investigated further for in vivo activity in preclinical models of METH self-administration as a potential treatment for METH use disorder.

Supplementary Material

Refer to Web version on PubMed Central for supplementary material.

Acknowledgments

This research was supported by DA013519, TR000117, TR001998 and GM109005 NIH grants, and an Arkansas Research Alliance (ARA) Scholar award. The University of Kentucky holds patents on the novel compounds described herein. A potential royalty stream to LPD and PAC may occur consistent with University of Kentucky policy.

References and notes

1. United Nations Office on Drugs and Crimes (UNODC). World Drug Report. 2004. http://www.unodc.org
2. Nordahl TE, Salo R, Leamon MJ. Neuropsychiatry Clin Neurosci. 2003; 15:317.
3. Iyo M, Namba H, Yanagisawa M, Hirai S, Yui N, Fukui S. Prog Neuropsychopharmacol Biol Psychiatry. 1997; 21:789. [PubMed: 9278950]
4. Barr AM, Panenka WJ, MacEwan GW, Thornton AE, Lang DJ, Honer WG, Lecomte T. J Psychiatry Neurosci. 2006; 31:301. [PubMed: 16951733]
5. Shoptaw SJ, Kao U, Heinzerling K, Ling W. Cochrane Database Syst Rev. 2009:CD003021. [PubMed: 19370579]
6. Darke S, Kaye S, McKetic R, Duflou J. Drug Alcohol Rev. 2008; 27:253. [PubMed: 18368606]
7. Shetty V, Mooney LJ, Zigler CM, Belin TR, Murphy D, Rawson R. J Am Dent Assoc. 2010; 141:307. [PubMed: 20194387]
8. Zheng G, Dwoskin LP, Crooks PA. AAPS J. 2006; 8:E682. [PubMed: 17233532]
9. Dwoskin LP, Crooks PA. Biochem Pharmacol. 2002; 63:89. [PubMed: 11841781]
10. Teng L, Crooks PA, Sonsalla PK, Dwoskin LP. J Pharmacol Exp Ther. 1997; 280:1432. [PubMed: 9067333]
11. Teng L, Crooks PA, Dwoskin LP. J Neurochem. 1998; 71:258. [PubMed: 9648873]
12. Court JA, Perry EK, Spurden D, Lloyd S, Gillespie JI, Whiting P, Barlow R. Brain Res. 1994; 667:118. [PubMed: 7534607]
13. Miller DK, Crooks PA, Zheng G, Grinevich VP, Norrholm SD, Dwoskin LP. J Pharmacol Exp Ther. 2004; 310:1035. [PubMed: 15121762]
14. Miller DK, Harrod SB, Green TA, Wong M, Bardo MT, Dwoskin LP. Pharmacol Biochem Behav. 2003; 74:279. [PubMed: 12479946]
15. Nickell JR, Zheng G, Deaciuc AG, Crooks PA, Dwoskin LP. J Pharmacol Exp Ther. 2011; 336:724. [PubMed: 20876747]
16. Zheng G, Dwoskin LP, Deaciuc AG, Norrholm SD, Crooks PA. J Med Chem. 2005; 48:5551. [PubMed: 16107155]
17. Neugebauer NM, Harrod SB, Stairs DJ, Crooks PA, Dwoskin LP, Bardo MT. Eur J Pharmacol. 2007; 571:33. [PubMed: 17612524]
18. Nickell JR, Culver JP, Janganati V, Zheng G, Dwoskin LP, Crooks PA. Bioorg Med Chem Lett. 2016; 26:2997–3000. [PubMed: 27212067]
19. Nickell JR, Culver JP, Janganati V, Zheng G, Dwoskin LP, Crooks PA. Bioorg Med Chem Lett. 2016; 26:4441. [PubMed: 27524311]
20. Joolakanti SR, Nickell JR, Janganati V, Zheng G, Dwoskin LP, Crooks PA. Bioorg Med Chem Lett. 2016; 26:2422. [PubMed: 27080180]
21. Nickell JR, Siripurapu KB, Horton DB, Zheng G, Crooks PA, Dwoskin LP. Behav Pharmacol. 2017; 795:143.
22. General synthetic procedure and analytical data for the fluoroethoxy-containing 1,4-diphenethylpiperidine and 1,4-diphenethylpiperazine analogs **(9a–9k & 15a–15f)**To compounds of general structure **8** or **14** (0.61 mmol) in DMF (5 mL), 2-fluoroethyltosylate (0.91 mmol) and

Cs_2CO_3 (0.91 mmol) were added at ambient temperature. Reaction mixtures were heated at 120°C for 6 h. After completion of the reactions (monitored by TLC), reaction mixtures were diluted with water and extracted with dichloromethane (2 × 30 mL). Organic layers were dried over Na_2SO_4 and concentrated under reduced pressure to afford crude products. Crude products were purified by column chromatography (silica gel, 3–5% methanol in dichloromethane) to afford pure products (yield 65–70%). These products were further converted to HCl salts by treatment with a 2M HCl solution in diethyl ether.4-(3-(2-fluoroethoxy)phenethyl)-1-phenethylpiperidine hydrochloride (**9a**)^{1}H NMR (CD_3OD, 400 MHz) δ 7.30–7.15 (m, 6H), 6.80–6.74 (m, 3H), 4.76 (t, J = 4.0 Hz, 1H), 4.64 (t, J = 4.0 Hz, 1H), 4.21 (t, J = 4.0 Hz, 1H), 4.14 (J = 4.0 Hz, 1H), 3.17 (d, J = 11.6 Hz, 2H), 2.88–2.84 (m, 2H), 2.76–2.72 (m, 2H), 2.64–2.60 (m, 2H), 2.27 (t, J = 11.2 Hz, 2H), 1.85 (d, J = 10 Hz, 2H), 1.61–1.56 (m, 2H), 1.39–1.33 (m, 3H) *ppm*. ^{13}C NMR (CD_3OD, 100 MHz) δ 160.1, 145.4, 140.4, 130.4, 129.6, 129.6, 127.4, 122.2, 115.8, 112.7, 84.0, 82.3, 68.5, 68.3, 61.2, 54.5, 39.1, 35.7, 33.9, 33.3, 32.2 *ppm*. HRMS (ESI) m/z calcd. for $C_{23}H_{31}FNO$ (M + H)$^+$ 356.2384, found 356.2393.4-(3-(2-fluoroethoxy)phenethyl)-1-(2-methoxyphenethyl)piperidine hydrochloride (**9b**)^{1}H NMR (CD_3OD, 400 MHz) d 7.14–7.06 (m, 3H), 6.85–6.79 (m, 2H), 6.73–6.68 (m, 3H), 4.69 (t, J = 3.6 Hz, 1H), 4.57 (t, J = 3.2 Hz, 1H), 4.12 (t, J = 4.0 Hz, 1H), 4.05 (t, J = 3.6 Hz, 1H), 3.73 (s, 3H), 3.01 (d, J = 10.8 Hz, 2H), 2.80–2.76 (m, 2H), 2.56–2.51 (m, 4H), 2.05 (t, J = 10.8 Hz, 2H), 1.71 (d, J = 8.8 Hz, 2H), 1.49 (s, 2H), 1.26 (s, 3H) *ppm*. ^{13}C NMR (CD_3OD, 100 MHz) δ 160.0, 158.7, 145.4, 131.2, 130.4, 128.8, 128.5, 122.2, 121.5, 115.8, 112.6, 111.4, 84.0, 82.3, 68.4, 68.2, 59.7, 55.7, 54.5, 39.1, 35.8, 33.9, 32.3, 28.2 *ppm*. HRMS (ESI) m/z calcd. for $C_{24}H_{33}FNO_2$ (M + H)$^+$ 386.2490, found 386.2504.4-(3-(2-fluoroethoxy)phenethyl)-1-(4-methoxyphenethyl)piperidine (**9c**)^{1}H NMR (CD_3OD, 400 MHz) δ 7.17–7.11 (m, 3H), 6.83–6.71 (m, 5H), 4.73 (t, J = 4.0 Hz, 1H), 4.61 (t, J = 4.0 Hz, 1H), 4.17 (t, J = 4.0 Hz, 1H), 4.10 (t, J = 4.0 Hz, 1H), 3.71 (s, 3H), 3.17 (J = 11.2 Hz, 2H), 2.81–2.73 (m, 4H), 2.57 (t, J = 8.0 Hz, 2H), 2.31 (t, J = 10.8 Hz, 2H), 1.81 (d, J = 10 Hz, 2H), 1.56–1.51 (m, 2H), 1.35–1.33 (m, 3H) *ppm*. ^{13}C NMR (CD_3OD, 100 MHz) δ 160.0, 159.7, 145.3, 131.7, 130.6, 130.4, 122.2, 115.8, 115.0, 112.7, 84.0, 82.3, 68.4, 68.2, 60.9, 55.6, 54.3, 38.8, 35.3, 33.8, 32.1, 31.8 *ppm*. HRMS (ESI) m/z calcd. for $C_{24}H_{33}FNO_2$ (M + H)$^+$ 386.2490, found 386.2501.4-(2-(2-fluoroethoxy)phenethyl)-1-phenethylpiperidine (**9d**)^{1}H NMR (CD_3OD, 400 MHz) δ 7.28–7.10 (m, 7H), 6.87 (t, J = 8.0 Hz, 2H), 4.75 (t, J = 3.6 Hz, 1H), 4.63 (t, J = 4.0 Hz, 1H), 4.17 (t, J = 4.0 Hz, 1H), 4.10 (J = 4.0 Hz, 1H), 3.11 (d, J = 11.2 Hz, 2H), 2.86–2.82 (m, 2H), 2.72–2.62 (m, 4H), 2.23 (t, J = 10.8 Hz, 2H), 1.82 (d, J = 10 Hz, 2H), 1.55–1.50 (m, 2H), 1.36–1.34 (m, 3H) *ppm*. ^{13}C NMR (CD_3OD, 100 MHz) d 157.6, 140.2, 132.2, 130.9, 129.6, 129.5, 128.1, 127.4, 122.0, 112.6, 84.0, 82.3, 68.7, 68.5, 61.0, 54.4, 37.6, 35.7, 33.2, 32.0, 28.3 *ppm*. HRMS (ESI) m/z calcd. for $C_{23}H_{31}FNO$ (M + H)$^+$ 356.2384, found 356.2390.4-(2-(2-fluoroethoxy)phenethyl)-1-(2-methoxyphenethyl)piperidine (**9e**)^{1}H NMR (CD_3OD, 400 MHz) δ 7.29–7.14 (m, 4H), 6.99–6.87 (m, 4H), 4.81 (t, J = 3.6 Hz, 1H), 4.69 (t, J = 4.0 Hz, 1H), 4.25 (t, J = 4.0 Hz, 1H), 4.18 (t, J = 4.0 Hz, 1H), 3.87 (s, 3H), 3.65 (d, J = 13.2 Hz, 2H), 3.25–3.21 (m, 2H), 3.08–3.04 (m, 2H), 2.97 (t, J = 12.4 Hz, 2H), 2.71 (t, J = 7.6 Hz, 2H), 2.09 (d, J = 13.6 Hz, 2H), 1.63–1.49 (m, 5H) *ppm*. ^{13}C NMR (CD_3OD, 100 MHz) δ 158.8, 157.7, 131.7, 131.5, 131.0, 129.9, 128.3, 125.4, 122.1, 121.9, 112.7, 111.7, 84.2, 82.5, 68.8, 68.6, 57.8, 55.8, 54.2, 37.4, 34.3, 30.8, 28.0, 26.6 *ppm*. HRMS (ESI) m/z calcd. for $C_{24}H_{33}FNO_2$ (M + H)$^+$ 386.2490, found 386.2499.4-(2-(2-fluoroethoxy)phenethyl)-1-(4-methoxyphenethyl)piperidine (**9f**)^{1}H NMR (CD_3OD, 400 MHz) δ 7.16–7.12 (m, 4H), 6.90–6.83 (m, 4H), 4.79 (t, J = 4.0 Hz, 1H), 4.67 (t, J = 4.0 Hz, 1H), 4.23 (t, J = 4.0 Hz, 1H), 4.16 (t, J = 4.0 Hz, 1H), 3.75 (s, 3H), 3.19 (d, J = 11.6 Hz, 2H), 2.84–2.65 (m, 6H), 2.32 (t, J = 10.8 Hz, 2H), 1.89 (d, J = 9.6 Hz, 2H), 1.59–1.54 (m, 2H), 1.39–1.35 (m, 3H) *ppm*. ^{13}C NMR (CD_3OD, 100 MHz) δ 159.6, 157.5, 132.0, 131.8, 130.7, 130.4, 127.9, 121.8, 114.8, 112.4, 83.9, 82.2, 68.6, 68.4, 61.0, 55.4, 54.3, 37.5, 35.6, 32.1, 31.9, 28.1 *ppm*. HRMS (ESI) m/z calcd. for $C_{24}H_{33}FNO_2$ (M + H)$^+$ 386.2490, found 386.2489. *1-(2-chlorophenethyl)-4-(2-(2-fluoroethoxy)phenethyl)piperidine (**9g**)*^{1}H NMR (CD_3OD, 400 MHz) δ 7.44–7.42 (m, 2H), 7.33–7.29 (m, 2H), 7.18–7.15 (m, 2H), 6.93–6.88 (m, 2H), 4.81 (t, J = 4.0 Hz, 1H), 4.69 (t, J = 3.6 Hz, 1H), 4.26 (t, J = 4.0 Hz, 1H), 4.19 (t, J = 4.0 Hz, 1H), 3.70 (d, J = 12.8 Hz, 2H), 3.32–3.23 (m, 5H), 3.03 (t, J = 12 Hz, 2H), 2.72 (t, J = 7.6 Hz, 2H), 2.11 (d, J = 11.6 Hz, 2H), 1.64–1.54 (m, 4H) *ppm*. ^{13}C NMR (CD_3OD, 100 MHz) δ 157.7, 135.2, 134.9, 132.3, 131.7, 131.0, 130.8, 130.2, 128.7, 128.3, 122.1, 112.7, 84.2, 82.5, 68.8, 68.6, 57.2, 54.2, 37.4, 34.3, 30.7, 29.2, 28.0 *ppm*. HRMS (ESI) m/z calcd. for $C_{23}H_{30}ClFNO$ (M + H)$^+$ 390.1994, found 390.1993.4-(2-(2-fluoroethoxy)phenethyl)-1-(4-fluorophenethyl)piperidine (**9h**)^{1}H NMR (CD_3OD, 400 MHz) d 7.26–7.23 (m, 2H), 7.16–7.13 (m,

2H), 7.02 (t, *J* = 8.4 Hz, 2H), 6.92–6.86 (m, 2H), 4.80 (t, *J* = 4.0 Hz, 1H), 4.68 (t, *J* = 4.0 Hz, 1H), 4.25 (t, *J* = 4.0 Hz, 1H), 4.18 (t, *J* = 4.0 Hz, 1H), 3.22 (d, *J* = 11.2 Hz, 2H), 2.90–2.77 (m, 4H), 2.69 (t, *J* = 7.2 Hz, 2H), 2.37 (t, *J* = 10 Hz, 2H), 1.92 (d, *J* = 9.6 Hz, 2H), 1.60–1.55 (m, 2H), 1.39–1.33 (m, 3H) *ppm*. ^{13}C NMR (CD_3OD, 100 MHz) *d* 164.3, 161.8, 157.7, 132.2, 131.4, 131.3, 131.0, 128.1, 122.0, 116.3, 116.1, 112.6, 84.1, 82.4, 68.8, 68.6, 60.9, 54.5, 37.7, 35.7, 32.3, 32.1, 28.3 *ppm*. HRMS (ESI) m/z calcd. for $C_{23}H_{30}F_2NO$ $(M + H)^+$ 374.2290, found 374.2300.1-(2-chlorophenethyl)-4-(4-(2-fluoroethoxy)phenethyl)piperidine (**9i**)^{1}H NMR (CD_3OD, 400 MHz) *d* 7.45–7.41 (m, 2H), 7.33–7.30 (m, 2H), 7.14–7.11 (m, 2H), 6.89–6.86 (m, 2H), 4.76 (t, *J* = 4.0 Hz, 1H), 4.64 (t, *J* = 4.0 Hz, 1H), 4.21 (t, *J* = 4.4 Hz, 1H), 4.14 (t, J = 4.4 Hz, 1H), 3.70 (d, *J* = 12.8 Hz, 2H), 3.32 (m, 4H), 3.03 (t, J = 12.4 Hz, 2H), 2.63 (t, *J* = 4.8 Hz, 2H), 2.08 (d, *J* = 12.4 Hz, 2H), 1.64–1.53 (m, 5H) *ppm*. ^{13}C NMR (CD_3OD, 100 MHz) *d* 158.3, 135.6, 135.1, 134.9, 132.3, 130.8, 130.3, 130.2, 128.7, 115.6, 84.0, 82.3, 68.7, 68.5, 57.2, 54.2, 38.7, 34.1, 32.7, 30.7, 29.2 *ppm*. HRMS (ESI) m/z calcd. for $C_{23}H_{30}ClFNO$ $(M + H)^+$ 390.1994, found 390.2010.1-(4-(2-fluoroethoxy)phenethyl)-4-phenethylpiperidine (**9j**)^{1}H NMR (CD_3OD, 400 MHz) *d* 7.24 (t, *J* = 4.0 Hz, 2H), 7.17–7.11 (m, 5H), 6.88 (d, *J* = 8.8 Hz, 2H), 4.74 (t, *J* = 4.0 Hz, 1H), 4.62 (t, *J* = 4.0 Hz, 1H), 4.19 (t, *J* = 4.0 Hz, 1H), 4.12 (t, *J* = 4.4 Hz, 1H), 3.11 (d, *J* = 11.2 Hz, 2H), 2.80–2.76 (m, 2H), 2.65–2.61 (m, 4H), 2.16 (t, *J* = 7.6 Hz, 2H), 1.82 (d, *J* = 10 Hz, 2H), 1.58–1.56 (m, 2H), 1.39–1.23 (m, 3H) *ppm*. ^{13}C NMR (CD_3OD, 100 MHz) *d* 158.6, 143.7, 133.2, 130.7, 129.3, 129.3, 126.7, 115.7, 84.0, 82.3, 68.7, 68.5, 61.6, 54.6, 39.4, 35.9, 33.9, 32.7, 32.5 *ppm*. HRMS (ESI) m/z calcd. for $C_{23}H_{31}FNO$ $(M + H)^+$ 356.2384, found 356.2395.1-(3-(2-fluoroethoxy)phenethyl)-4-phenethylpiperidine (**9k**)^{1}H NMR (CD_3OD, 400 MHz) *d* 7.27–7.14 (m, 6H), 6.91–6.84 (m, 3H), 4.76 (t, *J* = 4.0 Hz, 1H), 4.64 (t, *J* = 4.0 Hz, 1H), 4.24 (t, *J* = 3.6.0 Hz, 1H), 4.17 (t, *J* = 4.0 Hz, 1H), 3.64 (d, *J* = 12.8 Hz, 2H), 3.32–3.28 (m, 3H), 3.07–2.93 (m, 4H), 2.66 (t, *J* = 7.6 Hz, 2H), 2.05 (d, *J* = 13.2 Hz, 2H), 1.64–1.51 (m, 4H) *ppm*. ^{13}C NMR (CD_3OD, 100 MHz) *d* 160.5, 143.1, 139.3, 131.1, 129.4, 129.3, 126.9, 122.4, 116.3, 114.2, 84.0, 82.3, 68.6, 68.4, 59.1, 54.1, 38.6, 34.2, 33.6, 31.3, 30.7 *ppm*. HRMS (ESI) m/z calcd. for $C_{23}H_{31}FNO$ $(M + H)^+$ 356.2384, found 356.2394.1-(2-(2-fluoroethoxy)phenethyl)-4-phenethylpiperazine (**15a**)^{1}H NMR (CD_3OD, 400 MHz) *d* 7.37–7.26 (m, 7H), 7.03–6.95 (m, 2H), 4.91–4.89 (m, 1H), 4.79–4.77 (m, 1H), 4.36–4.34 (m, 1H), 4.29–4.26 (m, 1H), 4.09–3.58 (m, 7H), 3.54–3.47 (m, 5H), 3.20–3.14 (m, 4H) *ppm*. ^{13}C NMR (CD_3OD, 100 MHz) *d* 157.7, 137.1, 131.8, 130.2, 130.0 129.8, 128.4, 125.2, 122.6, 113.1, 84.2, 82.6, 68.9, 68.7, 31.2, 26.5 *ppm*. HRMS (ESI) m/z calcd. for $C_{22}H_{30}FN_2O$ $(M + H)^+$ 357.2337, found 357.2307.1-(3-(2-fluoroethoxy)phenethyl)-4-phenethylpiperazine (**15 b**)^{1}H NMR (CD_3OD, 400 MHz) d 7.37–7.24 (m, 7H), 6.96–6.93 (m, 2H), 4.76 (t, *J* = 4.0 Hz, 1H), 4.64 (t, *J* = 4.0 Hz, 1H), 4.23 (t, *J* = 4.0 Hz, 1H), 4.16 (t, *J* = 4.0 Hz, 1H), 4.09–3.59 (m, 7H), 3.54–3.47 (m, 5H), 3.18–3.08 (m, 4H) *ppm*. ^{13}C NMR (CD_3OD, 100 MHz) *d* 158.0, 135.7, 129.5, 128.6, 128.4, 127.9, 127.0, 114.7, 82.5, 80.8, 67.3, 67.1, 33.9, 29.7, 28.9 *ppm*. HRMS (ESI) m/z calcd. for $C_{22}H_{30}FN_2O$ $(M + H)^+$ 357.2337, found 357.2301.1-(4-(2-fluoroethoxy)phenethyl)-4-phenethylpiperazine (**15 c**)^{1}H NMR (CD_3OD, 400 MHz) *d* 7.38–7.26 (m, 6H), 6.96–6.87 (m, 3H), 4.78–4.76 (m, 1H), 4.66–4.64 (m, 1H), 4.27–4.20 (m, 1H), 4.20–4.18 (m, 1H), 4.11–3.59 (m, 7H), 3.55–3.48 (m, 5H), 3.17–3.11 (m, 4H) *ppm*. ^{13}C NMR ($CDCl_3$, 100 MHz) *d* 159.1, 137.3, 135.6, 129.7, 129.6, 128.6, 128.4, 127.0, 121.0, 119.3, 115.2, 114.9, 113.0, 82.5, 80.8, 67.2, 67.0, 29.7 *ppm*. HRMS (ESI) m/z calcd. for $C_{22}H_{30}FN_2O$ $(M + H)^+$ 357.2337, found 357.2348.1-(2-chlorophenethyl)-4-(2-(2-fluoroethoxy)phenethyl)piperazine dihydrochloride (**15d**)^{1}H NMR (CDCl3, 400 MHz) *d* 13.87 (brs, 1H), 13.62 (brs, 1H), 7.34–7.24 (m, 6H), 6.94 (d, *J* = 6.8 Hz, 1H), 6.84 (d, *J* = 7.6 Hz, 1H), 4.88 (s, 1H), 4.76 (s, 1H), 4.27–4.09 (m, 6H), 3.64 (brs, 4H), 3.44–3.25 (m, 8H) *ppm*. ^{13}C NMR ($CDCl_3$, 100 MHz) *d* 156.0, 133.8, 132.7, 131.2, 130.9, 130.0, 129.4, 129.2, 127.7, 123.8, 121.8, 111.8, 82.8, 81.1, 67.4, 56.5, 56.1, 48.3, 28.3, 25.7 *ppm*. HRMS (ESI) m/z calcd. for $C_{22}H_{29}ClFN_2O$ $(M + H)^+$ 391.1947, found 391.1947.1-(2-(2-fluoroethoxy)phenethyl)-4-(4-fluorophenethyl)piperazine dihydrochloride (**15e**)^{1}H NMR ($CDCl_3$, 400 MHz) *d* 13.87 (brs, 1H), 13.59 (brs, 1H), 7.29–7.20 (m, 4H), 7.02 (t, *J* = 8.4 Hz, 2H), 6.95 (t, *J* = 7.2 Hz, 1H), 6.86 (d, *J* = 8.4 Hz, 1H), 4.90 (s, 1H), 4.79 (s, 1H), 4.29–4.02 (7H), 3.68–3.59 (m, 4H), 3.31–3.24 (m, 7H) *ppm*. ^{13}C NMR ($CDCl_3$, 100 MHz) *d* 163.5, 161.1, 156.1, 131.4, 130.4, 129.6, 123.8, 122.1, 116.4, 111.9, 82.9, 81.2, 67.6, 58.3, 56.7, 48.3, 29.5, 25.9 *ppm*. HRMS (ESI) m/z calcd. for $C_{22}H_{29}F_2N_2O$ $(M + H)^+$ 375.2242, found 375.2215.1-(2-chlorophenethyl)-4-(4-(2-fluoroethoxy)phenethyl)piperazine (**15f**)^{1}H NMR ($CDCl_3$, 400 MHz) *d* 7.35–7.10 (m, 6H), 6.84 (d, *J* = 8.4 Hz, 2H), 4.78 (t, *J* = 4 Hz, 1H), 4.66 (t, *J* = 4 Hz, 1H), 4.20 (t, *J* = 4 Hz, 1H), 4.13 (t, *J* = 4 Hz, 1H), 2.95–2.91 (m, 3H), 2.76–2.72 (m, 3H), 2.62–2.54 (m, 10H) *ppm*. ^{13}C NMR (CD_3OD,

100 MHz) *d* 157.9, 133.6, 130.9, 129.6, 129.5, 129.0, 127.9, 127.4, 114.8, 82.5, 80.8, 67.3, 67.1, 29.0, 27.8 *ppm*. HRMS (ESI) m/z calcd. for $C_{22}H_{29}ClFN_2O$ $(M + H)^+$ 391.1947, found 391.1940.

23. Assay procedures for Vesicular [^{3}H]DA Uptake, Synaptosomal [^{3}H]DA, [^{3}H]5-HT Uptake and hERG Binding *Vesicular [^{3}H]DA Uptake Assays:* Inhibition of [^{3}H]DA (dihydroxyphenylethylamine,3,4-[7-^{3}H], 27.8 Ci/mmol; Perkin-Elmer) uptake was conducted using a preparation of isolated synaptic vesicles as previously described.[10,20] In brief, rat striata were homogenized with 10 up-and-down strokes of a Teflon pestle homogenizer (clearance ~ 0.003 inch) in 14 ml of 0.32 M sucrose solution. Homogenates were centrifuged (2000g for 10 min at 4°C) and the resulting supernatants were centrifuged again (10,000g for 30 min at 4°C). Pellets were re-suspended in 2 ml of 0.32 M sucrose solution and subjected to osmotic shock by adding 7 ml ice-cold water, followed by restoration of osmolality 5 min later by transferring suspensions to tubes containing 900 μl of 0.25 M HEPES buffer and 900 μl of 1.0 M potassium tartrate solution. Samples were centrifuged (20,000g for 20 min at 4°C) and the resulting supernatants were centrifuged again (55,000g for 1 h at 4°C), followed by the addition of 100 μl of 1.0 M $MgSO_4$, 100 μl of 0.25 M HEPES, and 100 μl of 1.0 M potassium tartrate solution before the final centrifugation (100,000g for 45 min at 4°C). Final pellets were re-suspended in 2.4 ml of assay buffer (25 mM HEPES, 100 mM potassium tartrate, 50 μM EGTA, 100 μM EDTA, 1.7 mM ascorbic acid, 2 mM ATP-Mg^{2+}, pH 7.4). Aliquots of the vesicular suspension (100 μl) were added to tubes containing assay buffer, various concentration of analog (1 nM to 0.1 mM) and 0.1 μM [^{3}H]DA to afford a final volume of 500 μl. Nonspecific uptake was determined in the presence of Ro4-1284 (10 μM). Reactions were terminated by filtration using a cell harvester (MP-43RS; Brandel Inc.) and radioactivity retained by Whatman GF/B filters (presoaked for 2 h in 0.5% polyethyleneimine) was determined by scintillation spectrometry.*Synaptosomal [^{3}H]DA and [^{3}H]5-HT Uptake Assays:* Analog-induced inhibition of [^{3}H]DA and [^{3}H]5-HT (5-hydroxytryptamine creatine sulfate 5-[1,2-^{3}H[N]], 29.5 Ci/mmol; Perkin-Elmer) uptake into rat striatal synaptosomes was determined using methods previously described.[20] Briefly, striata were homogenized in 20 ml of ice-cold 0.32 M sucrose solution containing 5 mM NaHCO3, pH 7.4, with 16 up-and-down strokes of a Teflon pestle homogenizer (clearance ~0.005 inch). Homogenates were centrifuged at 2000g for 10 min at 4°C, and resulting supernatants were centrifuged at 20,000g for 17 min at 4°C. Pellets were re-suspended in 1.5 ml of Krebs' buffer, containing 125 mM NaCl, 5 mM KCl, 1.5 mM $MgSO_4$, 1.25 mM $CaCl_2$, 1.5 mM KH_2PO_4, 10 mM a-d-glucose, 25 mM HEPES, and 0.1 mM EDTA, with 0.1 mM pargyline and 0.1 mM ascorbic acid, saturated with 95% O_2/5% CO_2, pH 7.4. Synaptosomal suspensions (20 μg of protein/50 μl) were added to duplicate tubes containing 50 μl of analog (1 nM to 0.1 mM, final concentration) and 350 μl of buffer and incubated at 34 °C for 5 min in a total volume of 450 μl. Samples were placed on ice, and 50 μl of [^{3}H]DA or [^{3}H]5-HT (10 nM, final concentration) was added to each tube for a final volume of 500 μl. Reactions proceeded for 10 min at 34 °C and were terminated by the addition of 3 ml of ice-cold Krebs' buffer. Nonspecific [^{3}H]DA and [^{3}H]5-HT uptake were determined in the presence of 10 μM GBR 12909 and 10 μM fluoxetine, respectively. Samples were rapidly filtered through Whatman GF/B filters. Filters were washed three times with 4 ml of ice-cold Krebs' buffer containing catechol (1 mM). Complete counting cocktail was added to the filters, and radioactivity was determined by scintillation spectrometry.*hERG Binding Assays:* Binding assays were conducted as described previously using membranes from HEK-293 cells, which specifically and stably express hERG channel protein (Millipore, Billerica, MA).[21,24] Briefly, cell membrane suspension (5 μg) was added to duplicate tubes containing assay buffer (50 mM Tris, 10 mM KCl, and 1 mM $MgCl_2$, pH 7.4), 25 μl of a single concentration (10 nM to 100 μM) of analog or amitriptyline (positive control)[25,26], and 25 μl (5 nM, final concentration) of [^{3}H]dofetilide (dofetilide [N-methyl-^{3}H], 80 Ci/mmol; American Radiolabeled Chemicals) for a final assay volume of 250 μl. Samples were incubated for 60 min at 25 °C and reactions terminated by rapid filtration through Whatman GF/B filters pre-soaked for 2 h in 0.5% polyethyleneimine. Filters were washed 3 times with 1 ml of ice-cold assay buffer. Radioactivity retained by the filters was determined by scintillation spectrometry.

24. Sviripa VM, Zhang W, Balia AG, Tsodikov OV, Nickell JR, Gizard F, Yu T, Lee EY, Dwoskin LP, Liu C, Watt DS. J Med Chem. 2014; 57:6083. [PubMed: 24950374]

25. Jo S-H, Youm JB, Lee CO, Earm YE, Ho WK. Br J Pharmacol. 2000; 129:1474. [PubMed: 10742304]

26. Teschemacher AG, Seward EP, Hancox JC, Witchel HJ. Br J Pharmacol. 1999; 128:479. [PubMed: 10510461]

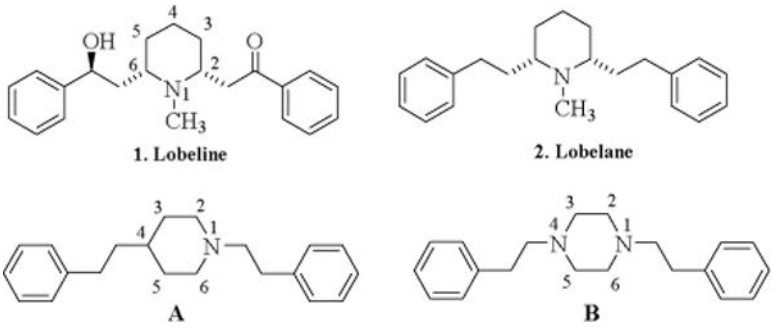

Figure 1.

Structures of lobeline (1), lobelane (2), which incorporate a 2,6-disubstituted piperidine scaffold. Structures A and B represent 1,4 disubstituted piperidine and piperazine scaffolds, respectively.

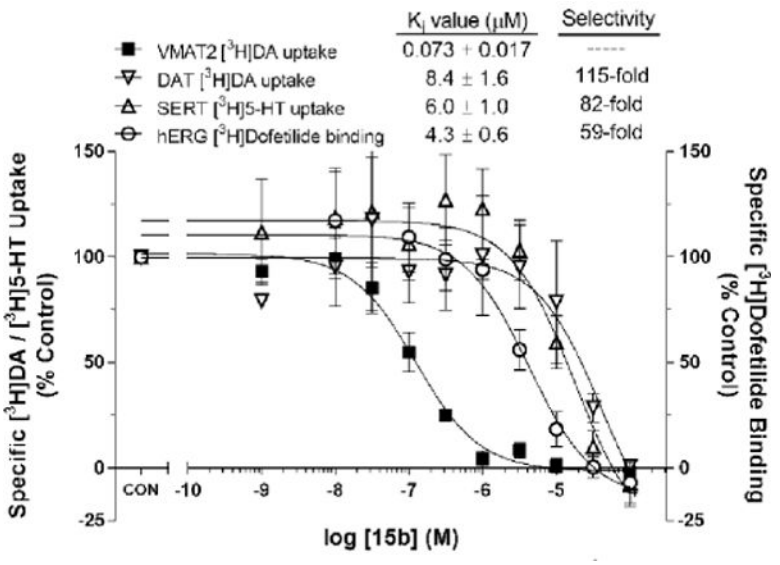

Figure 2.

Compound **15b** selectively inhibits specific [^{3}H]DA uptake into striatal vesicles relative to inhibition of [^{3}H]DA and [^{3}H]5-HT uptake into striatal synaptosomes and [^{3}H]dofetilide binding to the hERG channel protein in HEK-293 cells. Data are the mean (± S.E.M.) specific [^{3}H]DA or [^{3}H]5-HT uptake or [^{3}H]dofetilide binding presented as a percentage of the control condition (VMAT2 [^{3}H]DA uptake: 36.8 ± 11.8 fmol/mg; DAT [^{3}H]DA uptake: 13.4 ± 2.71 pmol/mg/min; SERT [^{3}H]5-HT uptake: 0.87 ± 0.25 fmol/mg; hERG [^{3}H]dofetilide binding: 1215.8 ± 353.0 fmol/mg; n=3–4 rats/uptake assay and 3 individual preparations of HEK-293 stock).

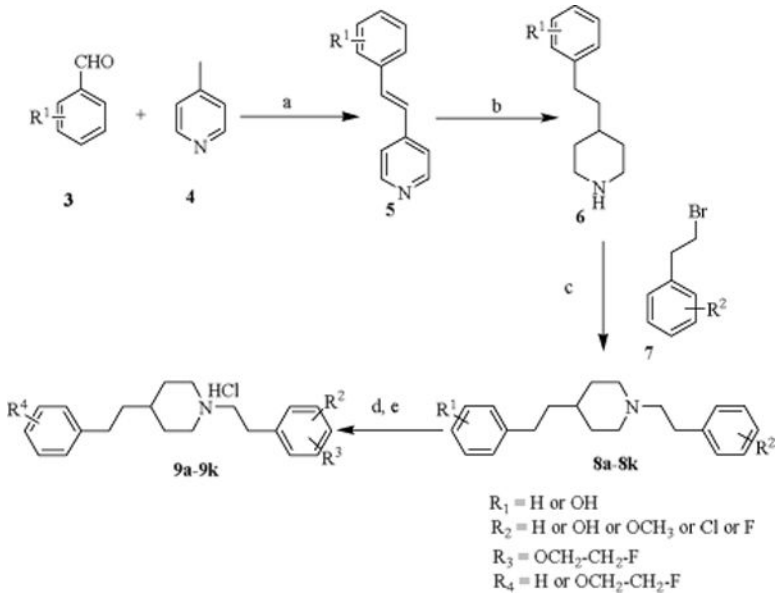

Scheme 1.

Synthesis of fluoroethoxy-substituted 1,4-diphenethylpiperidine analogs. *Reagents and conditions*: (a) Ac_2O, reflux, 24 h, 36–48%; (b) 10% (w/v) PtO_2/H_2, AcOH, 50 psi, rt,12 h, 75%; (c) K_2CO_3/acetonitrile, 80°C, 8 h, 75–80%; (d) F-CH_2-CH_2-OTs Cs_2CO_3, DMF/ reflux, 6 h, 65–70% (e) 2M HCl in diethyl ether.

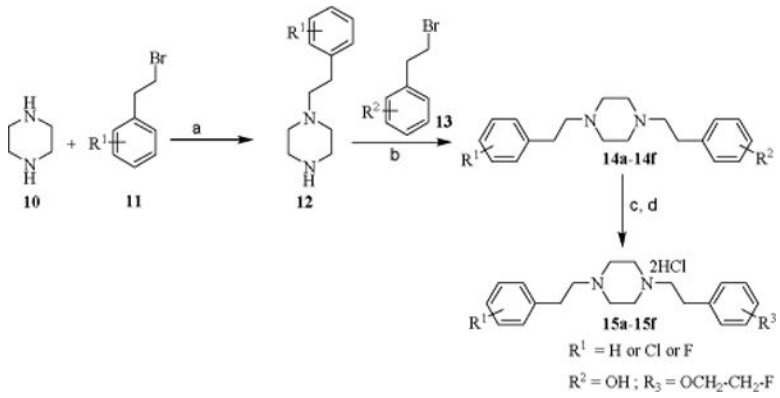

Scheme 2.

Synthesis of fluoroethoxy-substituted 1,4-diphenethylpiperazine analogs. *Reagents and conditions*: (a) toluene/reflux, 8–12 h, 70–75% (b) K_2CO_3/acetonitrile, 80°C, 8–10 h, 75–80%; (c) F-CH_2-CH_2-OTs, Cs_2CO_3, DMF/reflux, 6 h, 60–65% (d) 2M HCl in diethyl ether.

Table 1

Fluoroethoxy-containing 1,4-diphenethylpiperidine and 1,4-diphenethylpiperazine analog inhibition of [^{3}H]DA uptake at VMAT2 and DAT, [^{3}H]5-HT uptake at SERT, and [^{3}H]dofetilide binding

Compound	VMAT2 [^{3}H]DA Uptake K_i, μM	DAT [^{3}H]DA Uptake K_i, μM	SERT [^{3}H]5-HT Uptake K_i, μM	hERG [^{3}H]Dofetilide Binding IC50, μM
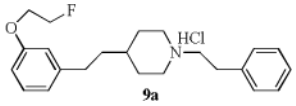 **9a**	0.053 ± 0.0059[a]	3.14 ± 0.16 (60-fold)[b]	2.41 ± 0.37 (46-fold)	0.75 ± 0.31 (14-fold)
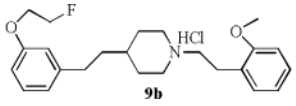 **9b**	0.061 ± 0.0052	4.79 ± 1.35 (79-fold)	0.47 ± 0.09 (8-fold)	0.80 ± 0.13 (13-fold)
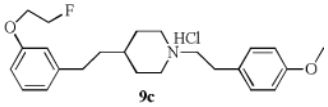 **9c**	0.067 ± 0.0020	3.70 ± 0.92 (56-fold)	0.66 ± 0.07 (10-fold)	0.28 ± 0.06 (4-fold)
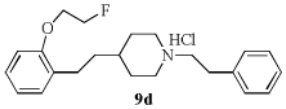 **9d**	0.035 ± 0.0043	2.75 ± 0.24 (78-fold)	5.68 ± 1.92 (161-fold)	0.76 ± 0.16 (22-fold)
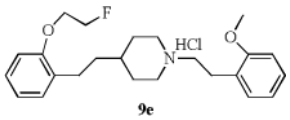 **9e**	0.025 ± 0.0017	2.31 ± 0.39 (94-fold)	1.16 ± 0.32 (47-fold)	0.43 ± 0.15 (17-fold)
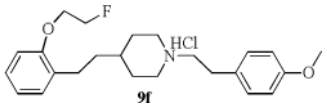 **9f**	0.073 ± 0.0058	5.58 ± 0.87 (77-fold)	2.13 ± 0.71 (29-fold)	0.35 ± 0.07 (5-fold)
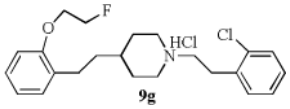 **9g**	0.062 ± 0.0033	2.76 ± 0.65 (45-fold)	1.45 ± 0.10 (24-fold)	0.69 ± 0.12 (11-fold)
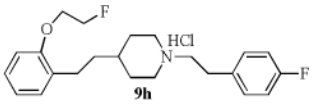 **9h**	0.027 ± 0.0028	2.14 ± 0.26 (78-fold)	3.66 ± 0.86 (134-fold)	0.38 ± 0.09 (14-fold)
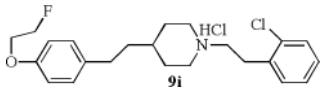 **9i**	0.19 ± 0.012	2.71 ± 0.57 (15-fold)	3.62 ± 0.95 (20-fold)	2.20 ± 0.65 (12-fold)
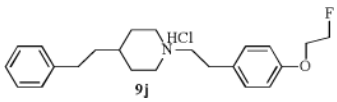 **9j**	0.15 ± 0.013	1.06 ± 0.04 (7-fold)	0.39 ± 0.09 (3-fold)	0.35 ± 0.16 (2-fold)

Compound	VMAT2 [^{3}H]DA Uptake K_i, μM	DAT [^{3}H]DA Uptake K_i, μM	SERT [^{3}H]5-HT Uptake K_i, μM	hERG [^{3}H]Dofetilide Binding IC50, μM
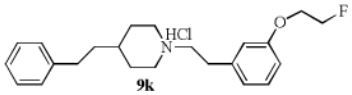 **9k**	0.024 ± 0.0047	1.96 ± 0.23 (81-fold)	0.47 ± 0.18 (19-fold)	0.41 ± 0.05 (17-fold)
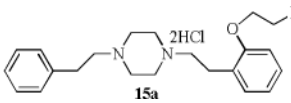 **15a**	0.035 ± 0.0046	4.57 ± 0.66 (130-fold)	0.26 ± 0.04 (7-fold)	5.49 ± 2.23 (156-fold)
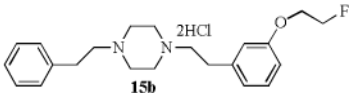 **15b**	0.073 ± 0.017	8.38 ± 1.61 (115-fold)	5.96 ± 1.01 (82-fold)	4.31 ± 0.63 (59-fold)
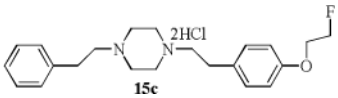 **15c**	0.60 ± 0.091	2.74 ± 0.13 (5-fold)	3.37 ± 0.81 (6-fold)	3.05 ± 0.93 (5-fold)
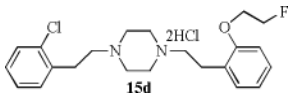 **15d**	0.014 ± 0.0026	2.24 ± 0.10 (160-fold)	0.072 ± 0.01 (5-fold)	0.85 ± 0.15 (61-fold)
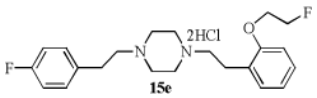 **15e**	0.024 ± 0.0027	1.57 ± 0.07 (65-fold)	0.30 ± 0.01 (13-fold)	1.12 ± 0.21 (47-fold)
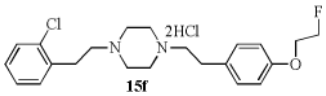 **15f**	0.45 ± 0.026	5.36 ± 0.12 (12-fold)	0.48 ± 0.04 (1-fold)	1.40 ± 0.34 (3-fold)

[a] Mean ± SEM for n=3–4/analog/assay

[b] Number within the parentheses represents fold selectivity relative to inhibition of VMAT2 function